Evidence of air-snow mercury exchange recorded in the snowpack at Dome Fuji, Antarctica

Yeongcheol Han   *School of Earth and Environmental Sciences/RIO, Seoul National University, Seoul 151-747, Republic of Korea*
                  Korea Polar Research Institute, Incheon 406-840, Republic of Korea
Youngsook Huh   *School of Earth and Environmental Sciences/RIO, Seoul National University, Seoul 151-747, Republic of Korea*
Sungmin Hong   *Department of Ocean Sciences, Inha University, Incheon 402-751, Republic of Korea*
Soon Do Hur*   *Korea Polar Research Institute, Incheon 406-840, Republic of Korea*
Hideaki Motoyama *National Institute of Polar Research, Tokyo 190-8518, Japan*

ABSTRACT: Measuring the mercury content in shallow Antarctic snow pits is useful for understanding the mercury dynamics of the Antarctic Plateau and the global mercury cycle and for interpreting ice core data. We determined the total mercury concentration (Hg_T) in snow samples successively collected at 5 cm intervals from two 4 m deep snow pits at Dome Fuji. The measured mercury concentration varied between 0.32 (the detection limit) and 2.93 pg g^{-1} (n = 160) with depth and was lower than that of summertime surface snow that was sampled simultaneously. This finding is consistent with previous observations that a bidirectional exchange of mercury between the snowpack and the atmosphere led to an increase in Hg_T in the surface snow during the summer. However, the contribution of the air-snow Hg exchange to the net Hg sequestration was offset by the intense re-emission of deposited mercury over the past ~50 years. Our results demonstrate that the Antarctic Plateau snowpack is a temporary reservoir of mercury rather than a permanent sink.

Key words: photochemical, Antarctic Plateau, Antarctic snow, total mercury

1. INTRODUCTION

The presence of mercury (Hg), an element of global concern, within the Antarctic Plateau snowpack and ice is important for two reasons. First, the Antarctic Plateau acts as a natural sink for mercury. Because of the vast area of the Antarctic Plateau (>5 million km^2), the amount of Hg sequestered in this region could account for a significant portion of the global mercury cycle (Brooks et al., 2008). Second, the variation in the mercury concentration with the snow depth can provide a temporal record of environmental changes that affect Hg sequestration (Vandal et al., 1993; Jiratu et al., 2009).

An active mercury exchange between the atmosphere and snowpack in the Antarctic Plateau has been observed to occur (Brooks et al., 2008; Dommergue et al., 2010). This observation has stimulated further research into the behavior of mercury in this region (Pfaffhuber et al., 2012; Dommergue et al., 2012; Han et al., 2011). One mercury species,

gaseous elemental mercury (Hg^0, GEM), has a relatively long atmospheric residence time of 6–24 months (Schroeder and Munthe, 1998), which allows it to be transported over long distances to the Antarctic Plateau. The snowpack in the Antarctic Plateau provides a large interstitial surface area for air-snow interactions (Dominé and Shepson, 2002), but Hg^0 interacts poorly with the snow surface (Bartels-Rausch et al., 2008; Ferrari et al., 2004). Instead, recent observations at the South Pole and Dome C suggest that the bidirectional exchange of mercury between the snowpack and the atmosphere is mediated by a change in its oxidation state via photochemical redox reactions (Brooks et al., 2008; Dommergue et al., 2012). For example, the deposition of atmospheric Hg was enhanced when reactive oxidized mercury (Hg^{II}) was abundant in the atmospheric boundary layer during the sunlit period (Brooks et al., 2008). On the other hand, Hg^0 flux from the snowpack to the atmosphere was observed during the summer, indicating that deposited Hg^{II} was reduced to Hg^0 within the snowpack and subsequently released into the atmosphere (Brooks et al., 2008; Dommergue et al., 2012). This bidirectional flux demonstrates active Hg cycling in the Antarctic Plateau, but it is unclear if this phenomenon occurs regularly and is widespread over this region.

Examining the Hg content in the snow can provide relevant information about the present-day behavior of mercury in the Antarctic Plateau and long-term trends in the Hg concentrations in Antarctic snow and ice. To date, there have been a few attempts to determine the mercury concentrations in the surface snow of the Antarctic Plateau (Han et al., 2011 and references therein). These concentrations were generally reported to range from less than 1 pg g^{-1} to a few pg g^{-1} (Han et al., 2011) before the photochemical behavior of mercury was recognized. In recent studies, highly elevated Hg concentrations indicated that atmospheric Hg^0 is photochemically oxidized to Hg^{II} and subsequently deposited onto the surface snow during the sunlit period (198 pg g^{-1} at the South Pole, Brooks et al., 2008; 60.3 pg g^{-1} near

Dome C, Dommergue et al., 2012).

We previously measured the total mercury concentration (Hg_T) in surface snow collected from Dome Fuji during the summer (Fig. 1) and did not observe any elevated concentrations (<0.4–10.8 pg g^{-1}, n = 30) (Han et al., 2011). Our results are inconsistent with observations from the other two dome sites (Brooks et al., 2008; Dommergue et al., 2012); however, these surface snow results cannot be directly compared for several reasons. First, the sampling thicknesses were not reported for most data. If the Hg concentration rapidly decreases with the snow depth, as reported by Brook et al. (2008), then sampling deeper snow layers will result in lower Hg concentrations. Second, the snow accumulation rate can vary between sites. In this case, samplings at the same depth will correspond to different time intervals at different sites, even within a small area (<0.01 km^2) (Kameda et al., 2008). Third, snow sampling has been typically conducted during the summer. Thus, the measured Hg concentration might differ depending on the rate of the photochemical air-snow Hg exchange during the sunlit period. Fourth, different analytical methods were used in these studies. The Hg concentration has been measured using: inductively coupled plasma sector field mass spectrometry (ICP-SFMS) (Han et al., 2011), cold vapor atomic fluorescence spectrometry (CVAFS) (Dommergue et al., 2012; Vandal et al., 1995) and photoacoustic Hg analysis (Sheppard et al., 1991). These analytical methods can produce different results. For example, it was shown that ICP-SFMS gave a higher total Hg concentration than cold vapor generation for the same snow samples. This result was attributed to the increased dissociation of non-reactive or strongly bound mercury with the ICP method (Planchon et al., 2004). The cold vapor generation method relies on the reduction of dissolved Hg^{II} to mercury vapor (Hg^0) using a reducing agent (e.g., $SnCl_2$, $NaBH_4$). Therefore, to determine the total mercury concentration, a pre-oxidation step involving an oxidant (e.g., BrCl) is required to solubilize all Hg in the sample prior to cold vapor generation. The data obtained without this pre-oxidation step only include labile mercury species, and the total mercury concentration is underestimated (Jiratu et al., 2009; Vandal et al., 1995). Therefore, systematic approaches for both sampling and analysis, which are required to properly trace the impact of mercury dynamics on the Antarctic Plateau snowpack, have rarely been used.

Here, following our previous study on the summer surface snow (Han et al., 2011), we report the Hg_T values for samples removed from two 4 m snow pits during the same expedition and measured using the same method as that used for the surface sample. These factors allowed us to reliably compare Hg_T of the surface snow and aged snow from the pits and to identify transient enhancement in the Hg deposition due to the air-snow Hg exchange during the sunlit period. Comparatively Hg-enriched surface snow can reveal the depositional enhancement of Hg during the sunlit

period and re-emission of the deposited Hg before being buried below the sunlit layer. In addition, measuring Hg_T in the successive snow layers could reveal temporal variations in Hg sequestration.

2. SAMPLE DESCRIPTION AND EXPERIMENTAL METHODS

2.1. Sample Description

Snow pits were dug at two sites in Dronning Maud Land, East Antarctica during the Japanese-Swedish Antarctic Expedition, which was executed between November 2007 and January 2008 as part of the International Trans-Antarctic Scientific Expedition (ITASE) (Fujita et al., 2011, 2012). Pit-A was located at Dome Fuji (77.30°S, 39.78°E, 3785 m), and Pit-B (75.88°S, 25.83°E, 3656 m) was located at a point ~400 km away from Pit-A (Fig. 1). Each pit was sampled successively at 5 cm intervals to a depth of 4 m by pushing a cylindrical sampling container horizontally. The snow samples were transported in pre-cleaned 500 mL LDPE bottles that were double-sealed in acid-cleaned LDPE bags and kept frozen in the dark until further processing. The ultraclean sampling protocol and cleaning procedure for the sampling materials are described in Hur et al. (2007) and Hong et al. (2000).

2.2. Analytical Procedures

The snow samples were aliquoted after melting at room temperature, but the two pits were treated differently. For
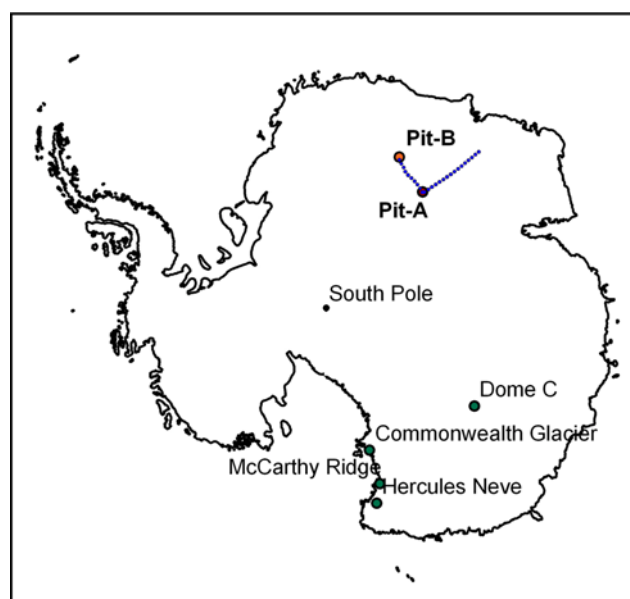

Fig. 1. The sampling locations for Pit-A at Dome Fuji and Pit-B (red circle). The blue dots are the sampling locations for the surface snow samples from Han et al. (2011). The green circles indicate the locations listed in Table 1.

Pit-A, ~5 mL samples were aliquoted into pre-cleaned 15 mL LDPE bottles and stored frozen in the dark. The aliquots were thawed and acidified with HNO_3 to 2% just prior to the analyses. For Pit-B, ~5 mL aliquots were transferred into 20 mL PFA bottles and acidified with HNO_3 to 2%. The Pit-B aliquots were analyzed within 24 hours and therefore did not require storage. Melting and aliquoting were performed in a class 10 clean bench at the Korea Polar Research Institute (KOPRI).

The difference in the aliquot preparation was due to potential mercury loss during this step. Mercury is unstable in dilute nitric acid and is readily volatilized (Han et al., 2011). Although mercury is sometimes stable in snowmelt (Planchon et al., 2004), we observed a significant Hg loss from the surface snow samples in our previous study, which resulted in an underestimation of Hg_T by a factor of 2–5 (Han et al., 2011). The Pit-A samples were handled in the same way as the surface snow samples during sampling, transport, storage, aliquoting and analysis. These processes might have resulted in a Hg loss from the Pit-A samples similar to those from the surface snow samples, meaning that comparisons between these samples should be valid. For Pit-B, to minimize the potential Hg loss, the aliquots were contained in Teflon (PFA) bottles that reduce Hg loss (Parker and Bloom, 2005), and these samples were analyzed immediately after aliquoting. The difference in the aliquot preparation provided another basis for comparing the Hg loss after the initial snow melting in the Pit-A and Pit-B samples.

Hg_T of the snowmelt samples was measured by inductively coupled plasma sector field mass spectrometry (ICP-SF-MS) using an Element2 instrument (Thermo Scientific, Bremen, Germany) at the National Center for Inter-university Research Facilities (NCIRF) at Seoul National University. ICP-SF-MS can quantify Hg at sub-pg g^{-1} levels with a small sample volume (<a few mL), which is particularly useful for typically small polar snow (or ice) samples. The details of the analytical method can be found in Han et al. (2011). To obtain the external calibration curves for ^{201}Hg and ^{202}Hg (natural abundances of 13.2% and 29.9%, respectively), working standard solutions were prepared by diluting a single Hg elemental standard with an initial concentration of 1000 mg L^{-1} in a 10% HNO_3 matrix (ICP standard, Merck) to between 1 to 50 pg g^{-1} in 2% (v/v) HNO_3. To prevent mercury loss in the dilute standard solutions, a gold chloride ($AuCl_3$) solution (final concentration of 100 μg L^{-1}) was added as a preservative. The instrumental sensitivity varied within 100–140 cps (pg g^{-1})$^{-1}$ ($r^2 > 0.998$) for ^{202}Hg over the course of our analyses, which resulted in slightly different detection limits of 0.36 pg g^{-1} and 0.32 pg g^{-1} for Pit-A and Pit-B, respectively. The detection limits were estimated to be three times the standard deviation of the blank signal (n = 9). To ensure the accuracy of the calibration, two different certified reference materials (CRM) were tested: (1) ORMS-4 (elevated Hg in river water, 22.0 ± 1.6 pg g^{-1}, stabilized with 0.5% (v/v) BrCl, NRCC) and (2) diluted (1:100,000) SRM 1641D (mercury in water, 1.557 ± 0.020 μg g^{-1}, acidified to 2% (v/v) HNO_3 and stabilized with 1 μg g^{-1} gold, NIST). Because ORMS-4 contains tungsten-186 (^{186}W), which interferes with ^{202}Hg detection, ORMS-4 was used as a reference material for ^{201}Hg. The diluted SRM 1641 was used to ascertain the accuracy of both the ^{201}Hg and ^{202}Hg concentrations. All CRM results were within 10% of the certified values.

The memory effect in the sample introduction compartment led to a low signal-to-blank ratio at the Hg pg g^{-1} level, but the blank contribution could be reliably subtracted from the total signal based on its short-term (1% RSD over 10 minutes) and long-term (10% RSD over the course of analysis, 470 ± 50 cps, n = 56) stability. The intensities of the ^{184}W and ^{185}Re signals were monitored for potential isobaric interference caused by their oxides ($^{186}W^{16}O$, $^{185}Re^{16}O$), but their contributions to the ^{202}Hg and ^{201}Hg signals were negligible for both the working standard solutions and snowmelt samples (less than 1%); hence, additional corrections were unnecessary.

Because, bottles opened at the sampling site could have adsorbed atmospheric Hg^{II}, which is abundant in the summer (Brooks et al., 2008), the unopened sample bottles brought to the sampling site were used as field blanks. The empty bottles were filled with deionized water in the laboratory and analyzed; no Hg was detected. In addition, several of the samples (63 out of 160) did not contain detectable amount of Hg, indirectly suggesting that contamination due to the snow sampling was negligible.

2.3. Depth-to-Age Models

The depth-to-age models for both snow pits were adopted from Soyol-Erdene et al. (2011) (Fig. 2), in which the non-sea-salt sulfate (nss-SO_4^{2-}) concentration was determined using aliquots from Pit-A and Pit-B. The depth-to-age relations were constrained by correlating striking nss-SO_4^{2-} anomalies to the large volcanic eruptions of Mt. Pinatubo (1991), Mt. Cerro Hudson (1991) and Mt. Agung (1963). Using linear interpolation, Pit-A and Pit-B were estimated to cover ~53 years (1955–2008) and ~34 years (1974–2008), respectively.

Based on the mean snow accumulation rates of ~8 and ~12 cm y^{-1} for Pit-A and Pit-B, respectively, a 5 cm snow layer corresponds to average time intervals of approximately 8 months in Pit-A and 5 months in Pit-B, which allows the examination of seasonal to interannual variations in Hg sequestration. However, on-site monitoring at Dome Fuji using 36 bamboo stakes showed wide spatial variations in the snow accumulation rate, ranging from 46% to 123% within an area of <0.01 km^2 from 1995 to 2006 (Kameda et al., 2008). These variations resulted from extremely low precipitation rates and intense post-depositional reworking,
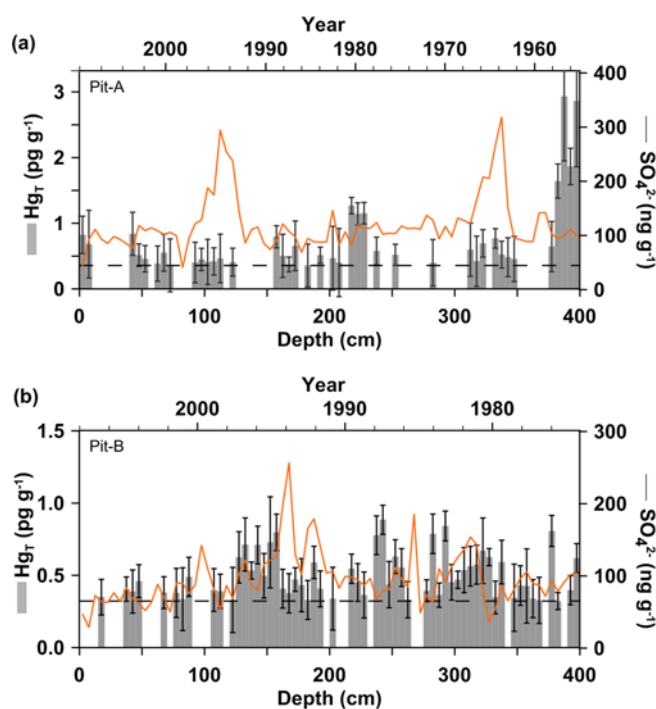
Fig. 2. The total mercury concentration (bars) profiles showing the 90% confidence intervals, sulfate concentration (line) and depth-to-age model (top). The horizontal dotted lines show the detection limits.

such as wind-blown redistribution or sublimation. Accordingly, the time period covered by a 5 cm snow layer might vary widely.

3. RESULTS

The Hg_T depth profiles with 90% confidence intervals are presented in Figure 2 and Appendix 1. The confidence intervals were calculated based on different instrumental replicates (5 to 20) with relative standard deviations ranging from 4 to 61% and averaging 22%. The results varied between <0.36 (below d.l., n = 40) and 2.93 pg g^{-1} in Pit-A (n = 80; Fig. 2a) and between <0.32 (below d.l., n = 23) and 0.89 pg g^{-1} in Pit-B (n = 80; Fig. 2b). All results were within the previously reported range but were at the low end of the range (Han et al., 2011). The aliquots from Pit-B were expected to suffer less Hg loss than those from Pit-A because they were placed in Teflon containers and analyzed immediately (Parker and Bloom, 2005; Han et al., 2011). However, both pits had a similar range in Hg_T, suggesting that original mercury contents in Pit-B were lower than those in Pit-A. By contrast, if the Hg loss was minimal for the snow pit melts (Planchon et al., 2004), rather than substantial as for the surface snow melts (Han et al., 2011), then the measured Hg_T might reflect the actual mercury contents in both pits.

Hg_T was lower in the snow pit samples than in the surface snow samples (Student's t-test; P < 0.01). The averages values (±standard deviation) for Pit-A and Pit-B were 0.5 (±0.5)
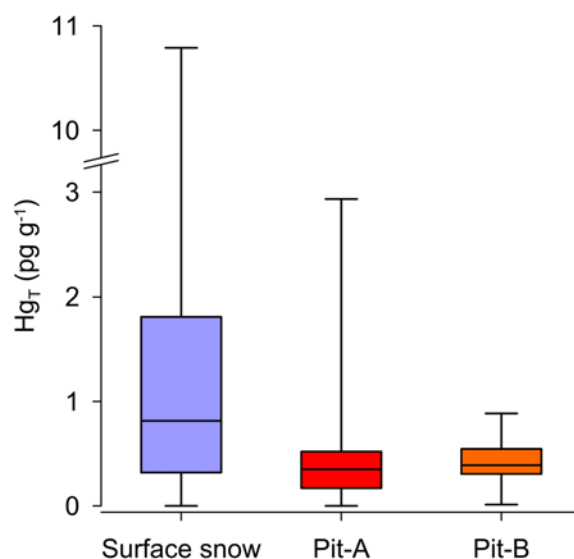

Fig. 3. The box-whisker plot for the surface snow samples (Han et al., 2011), Pit-A and Pit-B.

and 0.4 (±0.2) pg g^{-1}, respectively, whereas that of the surface snow samples from an altitude of >2500 m was 1.8 (±2.3) pg g^{-1} (n = 30). Box-whisker plots also illustrate the relative enrichment of Hg_T in the surface snow (Fig. 3). These results are consistent with the previous observation that Hg_T was anomalously high at the surface (198 pg g^{-1}) and rapidly decreased with depth (to <10 pg g^{-1}) at the South Pole in the summer (Brooks et al., 2008).

We calculated the mercury sequestration rates (pg cm^{-2} yr^{-1}) by multiplying the concentrations (pg g^{-1}) measured in the snow by the snow density (g cm^{-3}) at each depth. The snow density data were adopted from Fujita et al. (2012). The mercury sequestration rates were 0.6–2.0 pg cm^{-2} yr^{-1} for Pit-A and 1.1–2.4 pg cm^{-2} yr^{-1} for Pit-B during the ~53 and ~34 year time periods, respectively. However, these rates might have been underestimated because of the potential Hg loss.

The available mean mercury sequestration rates determined from Antarctic snowpack or ice cores are compiled in Table 1. The prehistoric Hg sequestration rate in the Antarctic Plateau was solely reconstructed from Dome C ice cores (Vandal et al., 1993; Jiratu et al., 2009) and was estimated to be ~6 pg cm^{-2} y^{-1} during the interglacial period (Jiratu et al., 2009). Recent Hg sequestration rates estimated from near-coastal sites in Victoria Land are 11 pg cm^{-2} y^{-1} (Witherow and Lyons, 2008) and 3.9 and 10.2 pg cm^{-2} y^{-1} (Capelli et al., 1998). The latter two values are likely underestimated because they were determined based on labile Hg species rather than Hg_T. In comparison, the rates at our sampling sites are among the lowest. The existing data indicate the mercury sequestration rates are higher at low-elevation coastal sites with high snow accumulation rates than at inland plateau sites, which are subject to extremely arid conditions.

Table 1. Mercury sequestration rates estimated from Antarctic snowpack or ice core

Location	Distance from coast (km)	Elevation (m)	Snow accumulation rate (cm y^{-1})	Recovered period	Hg concentration (pg g^{-1})	Hg sequestration rate (pg cm^{-2} y^{-1})	Analytical method	Sample type	Reference
Dome Fuji (Pit-A)	900	3785	8	1957–2007	<0.36 (d.l) –2.93	1.3	ICP-SF-MS	snow pit	this study
Dome Fuji (Pit-B)	650	3656	12.5	1975–2007	<0.32 (d.l) –0.89	1.9	ICP-SF-MS	snow pit	this study
Commonwealth Glacier, Taylor Valley, Victoria Land	10	678	15	1987–2004	0.3–40	11	CVAFS with oxidation	snow pit	Witherow and Lyons (2008)
Hercules Névé, Victoria Land	80	2960	38.6	1988–1993	0.09–0.55[a]	3.9	CVAFS without oxidation	snow pit	Capelli et al. (1998)
McCarthy Ridge, Victoria Land	40	875	55.0	1990–1993	0.16–0.71[a]	10.2	CVAFS without oxidation	snow pit	Capelli et al. (1998)
Dome C	1000	3240	–	3.9–33.7 ka	0.19–2.21[a]	0.9–3.1	CVAFS without oxidation	ice core	Vandal et al. (1993)
Dome C	1000	3233	–	2–672 ka	<1 (d.l)–65	<1–121	ICP-SF-MS	ice core	Jiratu et al. (2009)

[a]determined from the measurement of labile species without a pre-oxidation step.

4. DISCUSSION

The higher Hg$_T$ in the surface snow compared with the snow pits indicates that (1) Hg deposition is enhanced during the sunlit period (surface > snow pit) and that (2) deposited Hg undergoes re-emission before being buried below the surface layer (snow pit < surface), demonstrating Hg exchange between the atmosphere and snowpack. The current understanding of mercury dynamics in the Antarctic Plateau can explain our Hg$_T$ results. First, elevated Hg$_T$ in the surface snow during summer can be attributed to photochemically enhanced Hg deposition. The photochemical oxidation of Hg^0 in the atmosphere produces reactive Hg^{II}, which is easily deposited on the surface snow. The deposition of atmospheric Hg^{II} can be further enhanced by, e.g., heavy snowfall (Lalonde et al., 2002), a thick boundary layer depth (Brooks et al., 2008; Dommergue et al., 2010) and a high air-borne dust load (Jiratu et al., 2009). Second, the deposited mercury returns to the atmosphere, leading to the lower Hg$_T$ in the aged snow from the snow pits. After deposition, Hg^{II} is reduced to Hg^0 under solar irradiation and re-emitted into the atmosphere. The lifetime of Hg^{II} in the snowpack is estimated to be several hours (Dommergue et al., 2007) but can vary depending on the chemical and physical properties of the snow and on meteorological factors, which are not yet fully understood (Steffen et al., 2008). This bidirectional Hg flux, which was also observed at the other two dome sites, the South Pole (Brooks et al., 2008) and Dome C (Dommergue et al., 2012), provides evidence that although the photochemical air-snow mercury exchange exhibits spatio-temporal heterogeneity (Han et al., 2011), it is widespread over the Antarctic Plateau during the sunlit period.

Mercury sequestration in the Antarctic Plateau snowpack results from the imbalance between its deposition and re-emission rates. If the net Hg deposition (deposition–re-emission) is enhanced by photochemical processes during the sunlit period, Hg$_T$ in the snow pit profile will vary seasonally. To study the seasonal variation in Hg$_T$, we compared Hg$_T$ to the sulfate (SO$_4^{2-}$) concentration (Fig. 2) because Iizuka et al. (2004) reported that thin layers depleted in sulfate form on the surface snow during the summer. By sampling the snow pit with a 2 cm resolution, Iizuka et al. recovered all summer layers, which were characterized by lower sulfate contents than the neighboring layers. However, the relative sulfate depletion was only partially detected in our study because of the thicker sampling interval of 5 cm (Fig. 2). A few Hg$_T$ peaks appeared to accompany the relative sulfate depletion (e.g., at depths of 40 cm in Pit-A and 280 and 290 cm in Pit-B) (Fig. 2), indicating that Hg sequestration was enhanced in the summer layers. However, we did not observe a relationship between Hg$_T$ and the sulfate concentration (r = –0.2 and 0.2 for Pit-A and Pit-B, respectively), suggesting weak seasonality in Hg sequestration. If the photochemical air-snow mercury exchange of mercury occurs every year, then the weak seasonality implies that most of the deposited Hg^{II} is reduced and returns to the atmosphere and that the Antarctic Plateau snowpack is mostly a temporary reservoir rather than a long-term mercury sink (Brooks et al., 2008). The low snow accumulation rate in the Antarctic Plateau favors the re-emission of Hg^0 under solar radiation because it allows sufficient time for deposited Hg^{II} to be reduced before being buried below the sunlit layer. The effective sunlight penetration depth is greater than 10 cm in the arid Antarctic inland (King and

Simpson, 2001; Warren et al., 2006) and thus reaches beyond the annual snow accumulation of ~8 cm at Dome Fuji, explaining the low sequestration at Dome Fuji compared to that at the other sites listed in Table 1. In fact, the snow accumulation generally increases toward Antarctic coast, leading to rapid burial of deposited Hg below the sunlit layer at the coastal sites. Because the available data on short-term Hg variations in Antarctic snow are still very limited and were obtained using different analytical methods, a more systematic approach is required to further investigate the spatial variation in Hg sequestration.

Instead of undergoing photo-reduction and re-emission, Hg^{II} scavenged by dust particles can resist photo-reduction to some extent and be preferentially sequestered in the snowpack (Jiratu et al., 2009; Han et al., 2011). At the bottom of Pit-A, the high Hg_T values accompanied by relatively large errors are thought to be related to particle scavenging because particles introduce a high degree of uncertainty in ICP-SFMS (Fig. 2a) (Han et al., 2011). In addition, high concentrations of other trace metals (i.e., Pt, As, Mo, Sb and Tl) were also found below 380 cm and were ascribed to the volcanic eruption of Carrán-Los Venados in 1955 (Soyol-Erdene et al., 2011; Hong et al., 2012). Thus, volcanic input might be a possible source of particles or particulate mercury.

One of the remaining questions is whether the air-snow exchange occurs during every sunlit period. The exchange requires the presence of Hg^{II} at the air-snow interface. Two different sources have been suggested for Hg^{II} in the atmospheric boundary layer: it can be transferred from the free troposphere by airmass subsidence and vertical mixing (Brooks et al., 2008; Pfaffhuber et al., 2012) or produced *in situ* in the atmospheric boundary layer (Dommergue et al., 2012). In the former case, active air-snow Hg exchange can be expected to occur every year because the free troposphere can consistently supply Hg^{II}. In the latter case, however, the presence of an Hg^0 oxidizing agent might exert substantial control over the extent of air-snow Hg exchange. However, the lack of long-term monitoring for atmospheric mercury and poor understanding of the mercury redox pathway both in the atmosphere and in the snowpack make it difficult to answer this question at present.

We did not find any relationship between Hg_T and other components, such as major elements, trace metals (Hong et al., 2012) or platinum group elements (Soyol-Erdene et al., 2011), in the sample aliquots. For example, significant volcanic depositions from Pinatubo (1993–1994), Cerro Hudson (1991–1992), El Chinchon (1982) and Agung (1964–1965) resulted in distinct peaks in $nss-SO_4^{2-}$, aluminum and platinum group elements within the snow profiles (Soyol-Erdene et al., 2011), but their role in mercury sequestration is unclear, despite significant mercury emissions from large volcanic eruptions into the atmosphere (Pyle and Mather, 2003). The lack of a relationship between the sequestration of Hg and other components suggests that Hg sequestration relies more on the deposition efficiency, which is primarily governed by photochemical processes, than on the source emission strength and transport routes that strongly influence the sequestration of other components.

5. CONCLUSION

Two shallow snow pits recovered from Dome Fuji were depleted in Hg compared to the summertime surface snow, suggesting that the air-snow mercury exchange is widespread over the Antarctic Plateau during the summer as a consequence of photochemical redox processes. Over the past ~50 years, however, the air-snow Hg exchange was not observed to enhance Hg sequestration. If the exchange usually occurs during the sunlit period, then the deposited mercury must undergo significant re-emission. These findings emphasize that the Antarctic Plateau snowpack serves as a temporary sink and source of mercury rather than a permanent sink.

REFERENCES

Bartels-Rausch, T., Huthwelker, T., Jöri, M., Gäggeler, H., and Ammann, M., 2008, Interaction of gaseous elemental mercury with snow surfaces: laboratory investigation. Environmental Research Letters, 3, 045009.

Brooks, S., Arimoto, R., Lindberg, S., and Southworth, G., 2008, Antarctic polar plateau snow surface conversion of deposited oxidized mercury to gaseous elemental mercury with fractional long-term burial. Atmospheric Environment, 42, 2877–2884.

Capelli, R., Minganti, V., Chiarini, C., and De Pellegrini, R., 1998, Mercury in snow layers from the Antarctica. International Journal of Environmental Analytical Chemistry, 71, 289–296.

Dominé, F. and Shepson, P.B., 2002, Air-snow interactions and atmospheric chemistry. Science, 297, 1506.

Dommergue, A., Bahlmann, E., Ebinghaus, R., Ferrari, C., and Boutron, C., 2007, Laboratory simulation of Hg^0 emissions from a snowpack. Analytical and Bioanalitical Chemistry, 388, 319–327.

Dommergue, A., Barret, M., Courteaud, J., Cristofanelli, P., Ferrari, C.P., and Gallée, H., 2012, Dynamic recycling of gaseous elemental mercury in the boundary layer of the Antarctic Plateau. Atmospheric Chemistry and Physics, 12, 11027–11036.

Dommergue, A., Sprovieri, F., Pirrone, N., Ebinghaus, R., Brooks, S.,

Courteaud, J., and Ferrari, C.P., 2010, Overview of mercury measurements in the Antarctic troposphere. Atmospheric Chemistry and Physics, 10, 3309–3319.

Ferrari, C.P., Dommergue, A., Boutron, C.F., Jitaru, P., and Adams, F.C., 2004, Profiles of mercury in the snow pack at Station Nord, Greenland shortly after polar sunrise. Geophysical Research Letters, 31, L03401.

Fujita, S., Enomoto, H., Fukui, K., Iizuka, Y., Motoyama, H., Nakazawa, F., Sugiyama, S., and Surdyk, S., 2012, Formation and metamorphism of stratified firn at sites located under spatial variations of accumulation rate and wind speed on the East Antarctic ice divide near Dome Fuji. The Cryosphere Discussion, 6, 1205–1267.

Fujita, S., Holmlund, P., Andersson, I., Brown, I., Enomoto, H., Fujii, Y., Fujita, K., Fukui, K., Furukawa, T., Hansson, M., Hara, K., Hoshina, Y., Igarashi, M., Iizuka, Y., Imura, S., Ingwander, S., Karlin, T., Motoyama, H., Nakazawa, F., Oerter, H., Sjöberg, L.E., Sugiyama, S., Surdyk, S., Ström, J., Uemura, R., and Wilhelms, F., 2011, Spatial and temporal variability of snow accumulation rate on the East Antarctic ice divide between Dome Fuji and EPICA DML. The Cryosphere, 5, 1057–1081.

Han, Y., Huh, Y., Hong, S., Hur, S.D., Motoyama, H., Fujita, S., Nakazawa, F., and Fukui, K.,2011, Quantification of total mercury in Antarctic surface snow using ICP-SF-MS: spatial variation from the coast to Dome Fuji. The Bulletin of the Korea Chemical Society, 32, 4258–4264.

Hong, S., Lluberas, A., and Rodriguez, F., 2000, A clean protocol for determining ultralow heavy metal concentrations: Its application to the analysis of Pb, Cd, Cu, Zn and Mn in Antarctic snow. Korean Journal of Polar Research, 11, 35–47.

Hong, S., Soyol-Erdene, T.-O., Hwang, H.J., Hong, S.B., Hur, S.D., and Motoyama, H., 2012, Evidence of global-scale As, Mo, Sb, and Tl atmospheric pollution in the Antarctic snow. Environmental Science and Technology, 46, 11550–11557.

Hur, S.D., Cunde, X., Hong, S., Barbante, C., Gabrielli, P., Lee, K., Boutron, C.F., and Ming, Y., 2007, Seasonal patterns of heavy metal deposition to the snow on Lambert Glacier basin, East Antarctica. Atmospheric Environment, 41, 8567–8578.

Iizuka, Y., Fujii, Y., Hirasawa, N., Suzuki, T., Motoyama, H., Furukawa, T., and Hondoh, T., 2004, SO_4^{2-} minimum in summer snow layer at Dome Fuji, Antarctica, and the probable mechanism. Journal of Geophysical Research, 109, D04307.

Jitaru, P., Gabrielli, P., Marteel, A., Plane, J.M.C., Planchon, F.A.M., Gauchard, P.A., Ferrari, C.P., Boutron, C.F., Adams, F.C., Hong, S., Cescon, P., and Barbante, C., 2009, Atmospheric depletion of mercury over Antarctica during glacial periods. Nature Geoscience, 2, 505–508.

Kameda, T., Motoyama, H., Fujita, S., and Takahashi, S., 2008, Temporal and spatial variability of surface mass balance at Dome Fuji, East Antarctica, by the stake method from 1995 to 2006. Journal of Glaciology, 54, 107–116.

King, M.D. and Simpson, W.R., 2001, Extinction of UV radiation in Arctic snow at Alert, Canada (82°N). Journal of Geophysical Research, 106, 12499–12507.

Lalonde, J.D., Poulain, A.J., and Amyot, M., 2002, The role of mercury redox reactions in snow on snow-to-air mercury transfer. Environmental Science and Technology, 36, 174–178.

Parker, J.L. and Bloom, N.S., 2005, Preservation and storage techniques for low-level aqueous mercury speciation. Science of the Total Environment, 337, 253–263.

Pfaffhuber, K.A., Berg, T., Hirdman, D., and Stohl, A., 2012, Atmospheric mercury observations from Antarctica: seasonal variation and source and sink region calculations. Atmospheric Chemistry and Physics, 12, 3241–3251.

Planchon, F.A.M., Gabrielli, P., Gauchard, P.A., Dommergue, A., Barbante, C., Cairns, W.R.L., Cozzi, G., Nagorski, S.A., Ferrari, C.P., Boutron, C.F., Capodaglio, G., Cescon, P., Varga, A., and Wolff, E.W., 2004, Direct determination of mercury at the sub-picogram per gram level in polar snow and ice by ICP-SFMS. Journal of Analytical Atomic Spectrometry, 19, 823–830.

Pyle, D.M. and Mather, T.A., 2003, The importance of volcanic emissions for the global atmospheric mercury cycle. Atmospheric Environment, 37, 5115–5124.

Schroeder, W.H. and Munthe, J., 1998, Atmospheric mercury – An overview. Atmospheric Environment, 32, 809–822.

Sheppard, D.S., Patterson, J.E., and McAdam, M.K., 1991, Mercury content of Antarctic ice and snow: Further results. Atmospheric Environment, 25, 1657–1660.

Soyol-Erdene, T.-O., Huh, Y., Hong, S., and Hur, S.D., 2011, A 50-year record of platinum, iridium, and rhodium in Antarctic snow: volcanic and anthropogenic sources. Environmental Science and Technology, 45, 5929–5935.

Steffen, A., Douglas, T., Amyot, M., Ariya, P., Aspmo, K., Berg, T., Bottenheim, J., Brooks, S., Cobbett, F., Dastoor, A., Dommergue, A., Ebinghaus, R., Ferrari, C., Gardfeldt, K., Goodsite, M.E., Lean, D., Poulain, A.J., Scherz, C., Skov, H., Sommar, J., and Temme, C., 2008, A synthesis of atmospheric mercury depletion event chemistry in the atmosphere and snow. Atmospheric Chemistry and Physics, 8, 1445–1482.

Vandal, G.M., Fitzgerald, W.F., Boutron, C.F., and Candelone, J.-P., 1993, Variations in mercury deposition to Antarctica over the past 34,000 years. Nature, 362, 621–623.

Vandal, G.M., Fitzgerald, W.F., Boutron, C.F., and Candelone, J.P., 1995, Mercury in ancient ice and recent snow from the Antarctic. In: Delmas, R.J. (ed.), Ice Core Studies of Global Biogeochemical Cycles. Springer-Verlag, Berlin, Germany, p. 401–416.

Warren, S., Brandt, R., and Grenfell, T., 2006, Visible and near-ultraviolet absorption spectrum of ice from transmission of solar radiation into snow. Applied Optics, 45, 5320–5334.

Witherow, R.A. and Lyons, W.B., 2008, Mercury deposition in a polar desert ecosystem. Environmental Science and Technology, 42, 4710–4716.

Appendix 1. Total mercury concentration in each layer of Pit-A and Pit-B

Depth (cm)		Pit-A (pg g^{-1})			Pit-B (pg g^{-1})		
Top	Bottom	Concentration	90% CI[a]	Estimated top age	Concentration	90% CI[a]	Estimated top age
0	5	0.82	0.28	2008.0	–	–	2008.0
5	10	0.68	0.52	2007.4	–	–	2007.6
10	15	–[b]	–	2006.7	–	–	2007.2
15	20	–	–	2006.1	0.35	0.12	2006.7
20	25	–	–	2005.5	–	–	2006.3
25	30	–	–	2004.8	–	–	2005.9
30	35	–	–	2004.2	–	–	2005.5
35	40	–	–	2003.5	0.41	0.08	2005.0
40	45	0.84	0.33	2002.9	0.39	0.15	2004.6
45	50	0.51	0.17	2002.3	0.46	0.11	2004.2
50	55	0.46	0.20	2001.6	–	–	2003.8
55	60	–	–	2001.0	–	–	2003.3
60	65	0.39	0.27	2000.4	–	–	2002.9
65	70	0.55	0.28	1999.7	0.38	0.11	2002.5
70	75	0.36	0.40	1999.1	–	–	2002.1
75	80	–	–	1998.5	0.38	0.17	2001.6
80	85	–	–	1997.8	0.34	0.22	2001.2
85	90	–	–	1997.2	0.49	0.14	2000.8
90	95	0.40	0.31	1996.5	–	–	2000.4
95	100	0.45	0.17	1995.9	–	–	1999.9
100	105	0.41	0.34	1995.3	–	–	1999.5
105	110	0.42	0.21	1994.6	0.40	0.15	1999.1
110	115	0.46	0.37	1994.0	0.39	0.12	1998.7
115	120	–	–	1993.3	–	–	1998.2
120	125	0.41	0.21	1992.7	0.33	0.23	1997.8
125	130	–	–	1992.0	0.62	0.18	1997.4
130	135	–	–	1991.3	0.71	0.18	1997.0
135	140	–	–	1990.7	0.53	0.06	1996.5
140	145	–	–	1990.0	0.71	0.13	1996.1
145	150	–	–	1989.3	0.50	0.15	1995.7
150	155	–	–	1988.7	0.73	0.32	1995.3
155	160	0.79	0.17	1988.0	0.80	0.13	1994.8
160	165	0.50	0.33	1987.3	0.41	0.13	1994.4
165	170	0.37	0.11	1986.7	0.38	0.14	1994.0
170	175	0.66	0.38	1986.0	0.47	0.08	1993.6
175	180	–	–	1985.3	0.43	0.18	1993.2
180	185	0.36	0.33	1984.7	0.33	0.13	1992.7
185	190	–	–	1984.0	0.59	0.11	1992.3
190	195	0.51	0.12	1983.3	0.41	0.12	1991.9
195	200	–	–	1982.7	–	–	1991.5
200	205	0.47	0.48	1982.0	0.34	0.22	1991.0
205	210	0.40	0.52	1981.3	–	–	1990.6
210	215	–	–	1980.7	–	–	1990.2
215	220	1.27	0.13	1980.0	0.55	0.10	1989.8
220	225	1.14	0.17	1979.3	0.45	0.13	1989.3
225	230	1.15	0.16	1978.7	0.36	0.16	1988.9

Appendix 1. (continued)

Depth (cm)		Pit-A (pg g^{-1})			Pit-B (pg g^{-1})		
Top	Bottom	Concentration	90% CI[a]	Estimated top age	Concentration	90% CI[a]	Estimated top age
230	235	–	–	1978.0	–	–	1988.5
235	240	0.58	0.21	1977.3	0.78	0.13	1988.1
240	245	–	–	1976.7	0.89	0.10	1987.6
245	250	–	–	1976.0	0.44	0.16	1987.2
250	255	0.52	0.16	1975.3	0.63	0.12	1986.8
255	260	–	–	1974.7	0.55	0.13	1986.4
260	265	–	–	1974.0	0.33	0.13	1985.9
265	270	–	–	1973.3	–	–	1985.5
270	275	–	–	1972.7	–	–	1985.1
275	280	–	–	1972.0	0.39	0.08	1984.7
280	285	0.40	0.35	1971.3	0.79	0.14	1984.2
285	290	–	–	1970.7	0.36	0.08	1983.8
290	295	–	–	1970.0	0.84	0.10	1983.4
295	300	–	–	1969.3	0.45	0.12	1983.0
300	305	–	–	1968.7	0.47	0.06	1982.5
305	310	–	–	1968.0	0.54	0.16	1982.1
310	315	0.60	0.41	1967.3	0.56	0.14	1981.7
315	320	0.42	0.38	1966.7	0.57	0.13	1981.3
320	325	0.69	0.21	1966.0	0.67	0.23	1980.8
325	330	–	–	1965.3	0.63	0.06	1980.4
330	335	0.77	0.15	1964.7	0.35	0.11	1980.0
335	340	0.52	0.20	1964.0	0.59	0.15	1979.6
340	345	0.48	0.30	1963.3	–	–	1979.2
345	350	0.46	0.34	1962.7	0.35	0.23	1978.7
350	355	–	–	1962.0	0.43	0.14	1978.3
355	360	–	–	1961.3	0.43	0.26	1977.9
360	365	–	–	1960.7	0.34	0.13	1977.5
365	370	–	–	1960.0	0.33	0.16	1977.0
370	375	–	–	1959.3	–	–	1976.6
375	380	0.64	0.38	1958.7	0.81	0.11	1976.2
380	385	1.64	0.26	1958.0	0.32	0.06	1975.8
385	390	2.93	0.98	1957.3	–	–	1975.3
390	395	1.87	0.28	1956.7	0.40	0.10	1974.9
395	400	2.86	1.00	1956.0	0.62	0.10	1974.5

[a]CI is the confidence interval. CIs are presented for the results above the detection limits.
[b]The hyphen indicates that the mercury concentration was below detection limit.